OPTIMIZING EDM PROCESS PARAMETERS USING RSM METHOD LINKED WITH GREY RELATIONAL ANALYSIS AND ARTIFICIAL NEURAL NETWORKS

Abstract

Electro discharge machining is as of late perceived as one of the adaptable assembling innovations to ensure less surface roughness and high rate of material removal all through machining of aluminum composite materials. This work portrays a preliminary examination of a full factorial plan completed on aluminum composite material with EDM process by separating the machining boundaries like Pinnacle current, Heartbeat On Time , Heartbeat Off Time, Discharge Voltage, Hole Width and Oil Strain. To assess the ideal cutting circumstances the machined opening amount boundaries analyzed include Surface Roughness (SR) and Material Removal Rate (MRR). System utilized is the multi objective optimization utilizing Demonstrating and reasonable reenactment strategy to assess the ideal cutting circumstances for creating deformity free machining. Aluminum composite material machinability boundaries were upgraded; utilizing ANN strategies trial information is gathered and tried. Executing Dark Engendering Calculation utilizing info and instrument type, the Multi-Layer Perception model has been made. Surface Roughness and Material Removal Rate are yield boundaries of the machined parts on culmination of the exploratory test and ANN are associated with approving the outcomes developed and furthermore to decide the presentation of the framework under different circumstances inside the working reach.

Keywords: Electro Discharge Machine, Response Surface Methodology, Gray Relational Analysis, Artificial Neural Network

Authors

R. Rajesh
Associate Professor and Head
Department of Mechanical Engineering
Noorul Islam Centre for Higher Education
Kumaracoil,Tamilnadu, India.
rajesh2009@niuniv.com

M. Dev Anand
Professor and Dean
Department of Mechanical Engineering
Noorul Islam Centre for Higher Education
Kumaracoil,Tamilnadu, India.

K. S. Jai Aultrin
Associate Professor
Department of Mechanical Engineering
Noorul Islam Centre for Higher Education
Kumaracoil,Tamilnadu, India.

S. Raja
Associate Professor
Department of Mechanical Engineering
Noorul Islam Centre for Higher Education
Kumaracoil,Tamilnadu, India.

I. INTRODUCTION

Electro Discharge Machining (EDM) is a widely recognized electrical non-conventional machining process commonly employed in precision machining applications for intricate work pieces with complex geometries. Thermal erosion refers to a phenomenon in which electrically conductive material is disintegrated by an electrically generated flash. Both the electrode and the work piece must possess electrical conductivity. The flash is observed within a cavity containing a dielectric solution, situated between the apparatus and the work piece. The metal removal process, utilizing electrical and thermal energy, operates without any physical contact between the machinery and the work piece. The utilization of thermal energy to machine conductive parts, regardless of their hardness, is an exceptional aspect. Its notable advantage lies in its contribution to the modern industrial sector. Electrical Discharge Machining (EDM) effectively eliminates mechanical burdens, chatter, and vibration problems during the machining process by establishing a non-contact connection between the electrode and the work piece. In contemporary research, a miniature electrode has been developed to effectively create openings on curved surfaces with high inclinations, without the need for conventional drilling techniques. The emission of light, commonly referred to as the flash, occurs as a result of the gap between the work piece and the instrument. Improved surface roughness (SR) can be achieved by utilizing smaller holes. Composites are materials that consist of at least two constituents bonded together at the interface within the composite. Each constituent originates from a distinct parent material that exists prior to the formation of the composite. Metal Matrix Composites (MMCs) are materials in which at least one constituent is a metal or alloy that incorporates one or more reinforcing phases. Typical metal matrix composites (MMCs) exhibit a dense metallic lattice structure that is continuous with a rigid ceramic substrate. The prevailing grid materials include aluminum, magnesium, and titanium, whereas the renowned fortification materials comprise Silicon Carbide (SiC), Titanium Carbide (TiC), Titanium Boride (TiB2), Boron Carbide (BiC), and Alumina (Al2O3). The thickness of many Metal Matrix Composites (MMCs) is approximately 33% of that of steel, resulting in a significant increase in both tensile strength and structural integrity. In the machining of such materials, traditional assembly processes are being replaced by more advanced methods that employ various forms of energy to remove the material. This shift is necessitated by the complexity of machining these advanced materials using conventional techniques, which makes achieving high-quality surface finishes and tight tolerances challenging. The advancement of automation technology has led manufacturers to focus more on the manipulation and reduction in size of components composed of expensive and durable materials.

The plausibility of assessing a global optimal solution and its accuracy depends on the specific optimization modeling techniques employed to define the objective functions and constraints associated with the decision variables. Accurate and robust models of the cycle can compensate for a lack of understanding and inadequate depiction of the interaction component in its entirety. The primary task in the field of optimization is the development of an optimization model. The process involves representing an optimization problem as a mathematical model in a standard format, which can be easily addressed using Response Surface Methodology (RSM). The objective of this study is to optimize the electrical discharge machining (EDM) process. The goal function and constraints, as well as the number of targets and the significance of reaching them, depend on the result boundary SR

and information boundaries such as Peak Current (Ip), Pulse On Time (Ton), Pulse Off Time (Toff), Discharge Voltage, Hole Width, and Oil Tension. The machining of Al/10% SiCp was conducted, and the observed performances are evaluated.

II. LITERATURE SURVEY

Various researchers have conducted process parameter optimization for various types of Electrical Discharge Machining (EDM) on multiple occasions, employing diverse optimization models and solution techniques. The evaluations of aforementioned prior investigations encompass notable determinants, purposeful criteria, restrictions, variable thresholds, observations, and their inherent limitations. The findings were succinctly summarized in the subsequent manner: The scholarly work conducted by Kuldeep Ojha and colleagues in 2010 provides valuable insights into the field of Electrical Discharge Machining (EDM), specifically pertaining to the enhancement of Material Removal Rate (MRR). Additionally, their research sheds light on the underlying mechanisms involved in the process of material removal. Subsequently, Sen and Shan (2007), Gao et al. (2008), and Rao et al. (2009) employed a congruent approach in their respective studies, focusing on the modeling and optimization of the electrical discharge machining (EDM) process across various combinations of work piece and tool materials. According to the scholarly work conducted by Tolga Bozdana and colleagues in 2010, an empirical examination was undertaken to explore the process of electrical discharge machining (EDM) drilling, specifically focusing on the creation of Ø2mm apertures in Inconel718 utilizing a brass electrode. The impact of process parameters on process outputs was documented with respect to the minimum number of experiments conducted. The application of Response Surface Methodology (RSM) has been employed to undertake the mathematical modeling of the aforementioned process. The findings indicate that the model that has been developed possesses the capability to achieve dependable prognostication of empirical outcomes with a level of accuracy that is deemed satisfactory. According to the scholarly work conducted by Musraat Ali and colleagues in 2009, it was found that... Differential Evolution (DE) stands as a prominent and uncomplicated Evolutionary Algorithm (EA) that is widely recognized for its efficacy in optimizing functions of real values, particularly those that exhibit multiple modes. The scholarly work conducted by B.H. Yan and colleagues in 1999 delves into a comprehensive analysis of the distinctive attributes associated with micro holes and the minimal rate of wear exhibited by tool electrodes. The primary objective of this study is to achieve a micro-hole of utmost precision in carbide materials. To this end, the researchers meticulously examine the impact of altering the polarity, the shape of the tool electrode, and the rotational speed of said electrode. In their seminal work, Mahapatra et al. (2006) put forth a proposition to investigate various influential factors in the wire electrical discharge machining (WEDM) process. These factors encompass discharge current, pulse duration, pulse frequency, wire speed, wire tension, and dielectric flow rate. Additionally, the authors sought to explore the potential interactions between these factors, with the ultimate goal of optimizing material removal rate (MRR) while simultaneously minimizing surface roughness (SR). To achieve this, they employed the Taguchi method, a robust statistical approach widely utilized in experimental design and optimization. The study conducted by Qing GAO et al. in 2008 illustrates the utilization of Artificial Neural Network (ANN) and Genetic Algorithm (GA) in the development of a parameter optimization model. A neural network model employing the Levenberg-Marquardt algorithm has been established to represent the correlation between

mean reciprocal rank (MRR) and input parameters. Additionally, a genetic algorithm (GA) is employed to optimize these parameters, resulting in the achievement of optimal outcomes. The exhibited model demonstrates a commendable level of efficiency, as evidenced by the notable progress in Mean Reciprocal Rank (MRR) achieved through the utilization of meticulously optimized machining parameters. In the scholarly work conducted by Shabgard et al. (2009), a concerted effort was undertaken to formulate mathematical models that establish the interrelationships between the Material Removal Rate (MRR), Tool Wear Rate (TWR), and Surface Roughness (SR) in the context of machining parameters. Moreover, a comprehensive investigation was conducted to scrutinize the ramifications of machining parameters with regards to the enumerated technological attributes. According to the scholarly work conducted by Sushant Dhar and colleagues in 2007, it has been elucidated that the machining of aluminium matrix composites poses a formidable challenge owing to the existence of rigid and fragile ceramic reinforcements. Electrical Discharge Machining (EDM) is an eminent technique employed in the realm of material fabrication. This study endeavors to assess the impact of various factors, namely current (c), pulse-on time (p), and air gap voltage (v), on the material removal rate (MRR), tool wear rate (TWR), and radial over cut (ROC) during the electrical discharge machining (EDM) process of Al–4Cu–6Si alloy–10%weight SiCp composites. Linear programming can be employed to attain the most favorable circumstances that yield the highest Material Removal Rate (MRR) while concurrently minimizing the Tool Wear Rate (TWR) and Rate of Chip (ROC). The magnitudes of the MRR (Mean Reciprocal Rank), TWR (Time Weighted Return), and ROC (Rate of Change) exhibit a substantial augmentation in a non-linear manner as the current is intensified. In the study conducted by Puertas et al. (2003), the focus lies on the characteristics pertaining to surface quality and dimensional accuracy. These parameters hold significant importance in the determination of optimal process conditions and economic considerations. The authors, in their work titled "Optimization of Cutting Parameters for Electrical Discharge Machining (EDM) using Taguchi Method and Artificial Neural Network (ANN)", proposed a pragmatic approach to enhance the efficiency of the machining process. They put forth a method that aims to minimize the overall machining time by leveraging the principles of Taguchi Method and Artificial Neural Network. The aforementioned methodology exhibits not only a commendable level of cost-effectiveness and temporal efficiency, but also a notable degree of efficacy and precision in its examination of the various machining parameters. It has been observed that the magnitude of electric current exerts a significant influence on the overall duration of the machining process. Consequently, the utilization of this approach yields enhancements in performance attributes such as the reduction of total machining time. The study conducted by Sameh S. H in 2009 demonstrates the enhancement of a comprehensive mathematical model that effectively correlates the interactive and higher order manipulation of diverse EDM parameters using Response Surface Methodology (RSM). This model was developed by utilizing pertinent experimental data obtained through rigorous testing procedures. The mathematical models have been formulated utilizing the principles of Response Surface Methodology (RSM), incorporating empirical data obtained from real-world observations of the Electrical Discharge Machining (EDM) process applied to work pieces. An expedition was undertaken to conduct an analysis of the requisite control conditions pertaining to the management of Material Removal Rate (MRR), Electrode Wear Ratio (EWR), gap size, and Spark Rate (SR). In their scholarly work, Seung-Han Yanga et al. (2009) propose a methodology that is highly recommended for optimizing the selection of optimal process parameters in the context of Electrical Discharge

Machining (EDM). Systematic cutting experiments are conducted on a die-sinking machine, wherein various conditions of process parameters are meticulously examined. The utilization of this particular system model aims to optimize both the Maximum Retrieval Rate (MRR) and the Success Rate (SR) concurrently through the implementation of a Simulated Annealing (SA) scheme. In a scholarly publication by Ramezan Ali Mahdavi Nejad in 2011, a proposal was put forth with the objective of concurrently optimizing the surface roughness (SR) and material removal rate (MRR) of electrical discharge machining (EDM) parameters for silicon carbide (SiC). Due to the inherent contradiction within the output parameters, it is regrettably impossible to identify a singular amalgamation of machining parameters that would yield optimal machining performance. Artificial Neural Networks (ANNs) employing the back propagation algorithm is employed to replicate the underlying process. The utilization of a multi-objective optimization technique, specifically the non-dominating sorting genetic algorithm-II, has been employed to effectively optimize the given process. The effects of three crucial input parameters in the process, namely discharge current, pulse on time (Ton), and pulse off time (Toff), on the electrical discharge machining (EDM) of silicon carbide (SiC) are under consideration. A series of experiments have been conducted utilizing a diverse range of input parameters to facilitate the training and validation of the model. The scholarly work conducted by G. Krishna Mohana Rao et al. (2010) aims to optimize the hardness of the surface generated in die dipping EDM by taking into account the concurrent influence of multiple input parameters. The conducted experiments involved the utilization of Ti6Al4V, HE15, 15CDV6, and M-250 as test specimens. The peak current and voltage were systematically altered during the experimentation process, and the resultant values of hardness were subsequently measured and recorded. The scholarly work conducted by Majumder et al. (2012) suggests a thorough examination of the process parameters involved in electrical discharge machining (EDM) with the aim of optimizing them to achieve the lowest possible EWR (electrode wear ratio). The parameters employed in this investigation encompass spark-current, pulse-on duration, and pulse-off duration.The correlation between the rate of electrode wear and the various parameters involved in the machining process has been established through the utilization of Response Surface Methodology (RSM). The primary objective of this endeavor is to showcase the unique characteristics of the input process in Electrical Discharge Machining (EDM) and how it is influenced by various process parameters. These works exemplify a comprehensive examination of the mediating factor within the realm of Electrical Discharge Machining (EDM) applied to materials, specifically Aluminum alloy with HE9 and LM25 Al/15%SIC. The examination of the Mean Reciprocal Rank (MRR) and Success Rate (SR) was undertaken. A total of six parameters underwent modifications throughout the course of the experiments. The empirical findings demonstrate that the primary factor influencing the material removal rate (MRR) is the magnitude of the electric current. Multiple researchers have presented the categorization of diverse research domains within the field of Educational Data Mining (EDM) and have also proposed potential avenues for future research, as depicted in Figure 1.The retrospective examination of literature has revealed and illuminated the fact that no literary compositions were executed in the domain of electronic dance music (EDM) utilizing an alloy of aluminum with 10% silicon carbide particles (Al/10% SiCp), and incorporating more than three variables. In their seminal work, Wang et al. (2016) devised and employed a pulse counting technique to meticulously scrutinize the alternating current trajectory during discharge, with the primary objective of elucidating the ramifications of reverse current. The phenomenon of reverse current flow serves a dual purpose, namely the

refinement of edges and the formation of a crater. The optimization of tool wear in relation to the removal of the work piece is achieved through the implementation of a diode, strategically positioned between the spark tracks of the discharging circuit, effectively circumventing the reverse current.

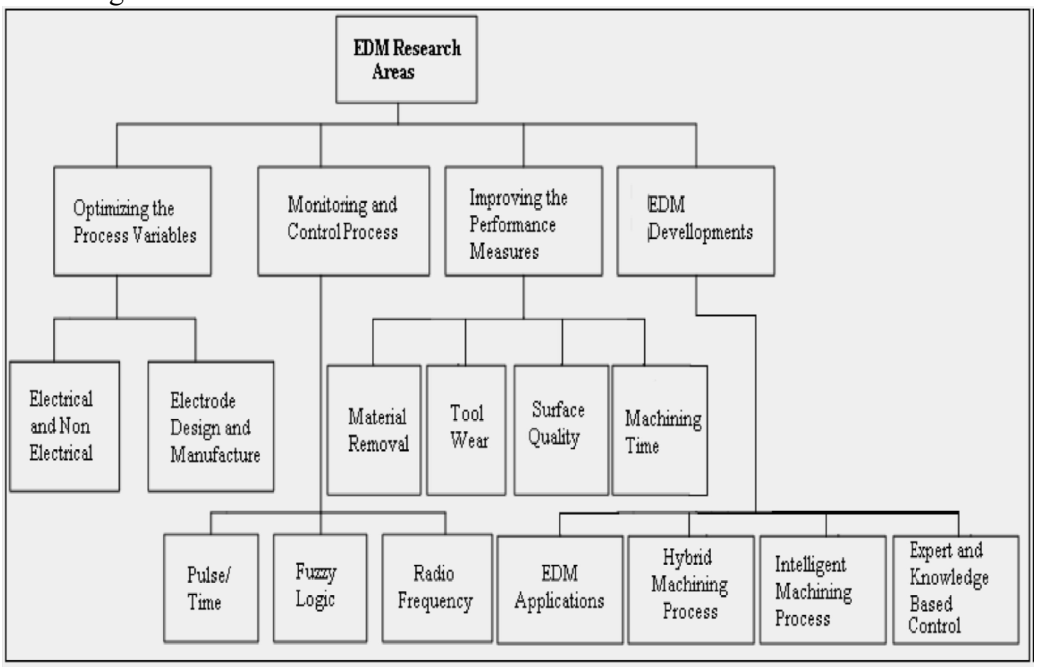

Figure 1: Classification of Major EDM Research Areas

III. EXPERIMENTAL DETAILS

A multitude of analyses were conducted to examine the performance and investigate the effects of different machining parameters in the EDM process on MMC in the fabrication of rectangular test specimens. The aforementioned examinations have been duly acknowledged for their endeavor to explore the ramifications of Peak Current (Ip), Discharge Voltage (V), Spark Gap, Pulse on Time (Ton), Pulse Off Time (Toff), and Oil Pressure (Poil) on SR. It is noteworthy that these parameters are regarded as plan variables within the context of this optimization process. The initiation of an optimization problem commences with the meticulous arrangement of the latent variables, which exhibit substantial disparities throughout the course of the optimization endeavor. The constraints embody intentional connections between the variables of the plan and other elements that pertain to the actual phenomenon being addressed. Additionally, certain assets possess greater significance or are considered equivalent to a particular asset value. Within the context of this particular endeavor, the factors of oversize and the EDM (Electrical Discharge Machining) opening are being regarded as limiting conditions or constraints.

1. **Work Material:** The Al-10% SiCp (Metal Matrix Composite) workpiece was fabricated using the technique of composite casting, meticulously measured and selected for its rectangular form with dimensions of 120mm x 120mm x 8mm. The material in question is selected due to its vast potential for application in the realm of manufacturing tools

within the shape industries. Furthermore, it has proven to be highly effective in the aeronautical and automotive sectors, owing to its exceptional strength-to-weight ratio and superior mechanical and physical properties when compared to conventional materials. Table-1 presents a comprehensive overview of the physical and mechanical properties pertaining to the Al-10% SiCp metal matrix composite (MMC) material. Table-2 presents a comprehensive depiction of the intricate chemical synthesis process employed in the production of the Al-10% SiCp Metal Matrix Composite (MMC) material.

Table 1: Physical and Mechanical Properties of Al-10% SiC_p MMC

Material	Density (gms/cm^3)	Tensile Strength (N/mm^2)	Hardness (BHN)	Modulus of Elasticity ($x10^3 N/mm^2$)	% Elongation
Al-$SiC10_p$	2.68	275	110	90	1.2 – 1.8

Table 2: Chemical Composition of Al-10% SiC_p MMC

Work Material	LM 25 Al-$SiC10_p$
Mg (%)	0.45
Si(%)	7.5
Cu(%)	0.2
Mn (%)	0.1
Fe (%)	0.2
Zn (%)	0.1
Ti (%)	0.2
SiC (%)	10
Reinforcement	10% SiC_p Particles (by Volume)
Particle Size (µm)	20

2. **Tool Material**: A cylindrical unadulterated copper with a diameter of 10mm was used as a tool cathode and it is utilized to puncture the work piece to 1mm profundity according to ISO specification cutting and tool holder M16 type were utilized for the manufacturing trials under various setting condition.

IV. FABRICATION OF COMPOSITE

The casting process with its initial stage is to put 90% aluminium LM25 metal into the vertical muffle furnace and set a temperature of 900°C from initial stage. After reaching the 900°C temperature the solid metal was melted and then 10% of powdered SiC_p is supplemented to it for removing slag formed in furnace. Then the molten metal is poured into the die. The die used for casting is rectangular die. Then the die is divided and finished Aluminium LM25 10% SiC composite material is taken. The desired end product composition is Mg .45%, Si 7.5%, Cu -.2, Mn.1, Fe .2, Zn .1, Ti .2,SiC 10%.

1. **Sintering:** Figure 2 shows the stir casting furnace and die their specifications are given below. Figure 3 shows the fabricated aluminum composite material.

Furnace Type	: Stir Casting Furnace
Load Voltage	: 100 Volt
Load Current	: 7 to 8 Amps
Melting Temp: Lm25 Al-alloy	: 900˚C
SiC	: 1400 ˚C
Degassing Tablet	: To remove moisture and gases
Soaking Time	: 3 Hours
Stir Rate	: 300 rpm

Figure 2: Stir Casting Furnace and Die

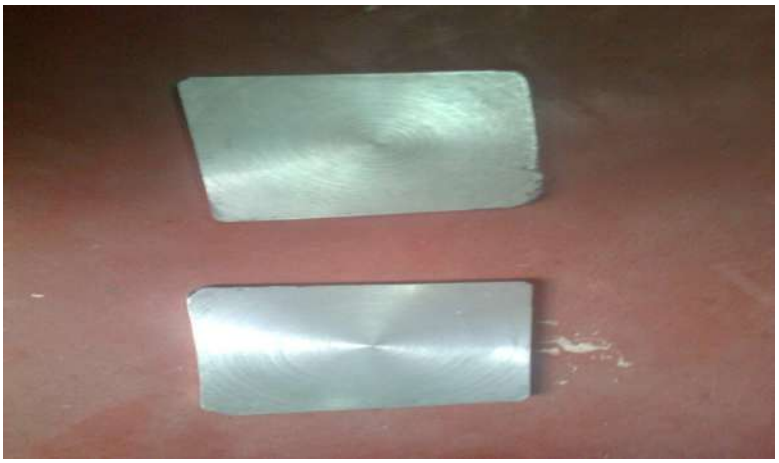

Figure 3: Al-10%SiC_p Composite Material

2. **EDM Machine:** With Electronica 5030 Die Sinking EDM machine experiments were conducted as shown in Figure 4. The dielectric fluid and electrode flushing method was utilized. The design of experimental conditions for EDM is depicted in Table 3.

Figure 4: Electronica 5030 Die Sinking EDM Machine

Table 3: EDM Machining Conditions

Conditions	Descriptions
Machine	Electronica 5030 die sinking EDM machine
Test Specimen	Composite Material (Mg .45%, Si 7.5%, Cu -.2, Mn.1, Fe .2, Zn .1, Ti .2, SiC 10%)
Tool	Copper Electrode of Diameter 10mm

Tool Polarity	Positive
Dielectric Fluid	EDM Oil (DEF-92)
Flushing Type	External
Depth of Cut (mm)	1
Electrode Polarity	Positive
Dielectric Flushing	Injection Flushing
Weight Measuring Instrument	Digital Balance (FX-3000)
SR Measuring Instrument	Portable SR Tester SJ201
Technical Data	**Co-Ordinate Table**
Supply Voltage : 415V, 3Ph.,50Hz	Mounting Surface (l*b) : 500*300mm
Taps : 380V, 415V, 440V	Maximum Workpiece Height : 175mm
Power Factor : 0.8 Approx	Maximum Workpiece Weight : 175kg
Height : 2075mm	Longitudinal Travel (X-axis) : 280mm
Width : 1230mm Depth : 1035mm	Transverse Travel (Y-axis) : 200mm
Net Weight : 800Kg (Approx.)	L.C of Hand Wheel Graduations with Vernier Scale : 0.005mm
	Width of Work Tank – Internal : 725mm
	Depth of Work Tank – Internal : 415mm
	Height of Work Tank : 315mm
Working Parameters	
Machining Current Max.: 35 Amps	Pulse Current : 2Amps
Open Gap O/V : 140 ± 5%	Current Range Selection : 10 Selection
	1 = 1Amp 2 = 2Amps 3-10 = 4Amps
Pulse Current : 2 Selection	Pulse On Duration : 2 to 1000µs
1 = 1Amp 1 = 1 Amp	
Weight : 250 Kg. (Approx.)	

V. EXPERIMENTAL PROCEDURE

As shown in Figure 5, ELECTRONICA EMS5030's machining system mounts the work piece on a V-block on an appealing table. Dial measure was used to test the device's

placement in the holder. To analyze variance, 54 runs with different parameter mixtures were used.

Figure 5: Electronica 5030 Die Sinking EDM Machining Process Underway

VI. MEASUREMENT PROCEDURE

The utilization of the Portable Roughness Tester SJ201 has facilitated the quantification of roughness, as visually depicted in Figure 6. The aforementioned device is a compact and autonomous apparatus designed for the purpose of assessing and quantifying the characteristics of surface texture. The parameters are executed based on the underlying chip architecture. The LCD screen serves as a visual display, presenting estimations and facilitating the diversion of results through the utilization of an optical printer or an additional computer, thereby enabling supplementary evaluation. The utilization of a non-battery-powered soluble battery facilitates the provision of electrical energy. Furthermore, it is equipped with a Jewel pointer that possesses a tip diameter measuring 5 micrometers. Commencing from a position of utmost eccentricity, the process of estimating commences in a manner that is universally applicable.

Throughout the duration of the estimation process, the pickup returns to its initial position in preparation for the subsequent estimation. The selection of the extracted magnitude determines the extent of the traversal. Perpetually, it is evident that the extent of traversal surpasses the predetermined threshold by a significant factor. Nevertheless, the amplification component can be duly calibrated. The profile meter has been configured with a predetermined threshold of 0.8mm, specifically for channel 2CR. The traverse speed has been set at 1mm/sec, while the traverse length spans 4mm. The roughness measurements, taken in the traverse bearing, have exhibited repetitive patterns across multiple work pieces. Specifically, the normal values of the SR parameter have been meticulously recorded for four distinct measurements.

Figure 6: Experimental Setup for Measuring Roughness

VII. EXPERIMENTAL SET-UP

The experiments were conducted under various machining conditions employing the Electronic 5030 Die Sinking Electrical Discharge Machining (EDM) apparatus, boasting a power output of 3HP/2.2KW. By configuring the machinery and determining the condition of the external layer of the work piece, the informational boundary was obtained. The tests were conducted using the conventional methodology as illustrated above. In the process of ascertaining the levels for each process boundary, it was observed that the boundary levels were found to be in accordance with the ranges suggested by the manufacturer of the machining equipment, as well as through careful examination of the existing survey. Out of the 54 conducted tests, it was observed that there are three distinct levels, each comprising six process parameters that are closely associated with the machining operation. The utilization of the SR tester SJ201 is employed in order to assess the work piece following each test, thereby determining the SR. The aforementioned table, denoted as Table 5, presents a comprehensive depiction of the perceptions pertaining to the examination and studies of helpers. Given the current conditions of the planning grid, it appears that the machining activities were executed in a rather haphazard manner with the intention of achieving precise measurements devoid of any errors.

Table 4: Different Variables Used in the Experiment and Their Levels

Variable	Coding	Level		
		1	2	3
Discharge Voltage (V) in V	A	60	65	70
Discharge Current in A	B	5	10	15
Pulse on time (T_{on})in s	C	15	30	45
Pulse off Time (T_{off}) in s	D	5	7	9

Spark gap (G) in mm	E	0.1	0.2	0.3
Oil Pressure in kg/cm^2	F	1	1.5	3

Next, plan RSM experiments using a Box Behnken technique with six variables. Table 5 shows the total number of machining parameter and recorderd SR tests.

Table 5: Planning Matrix of the Experiments with the Optimal Model Data

Sl. No.	A Voltage (V)	B Current (A)	C Pulse on Time (sec)	D Pulse off Time (sec)	E Gap Width (mm)	F Oil Pressure (Kg/cm^2)
1.	65	5	15	7	0.3	1.5
2.	75	10	45	7	0.2	2.0
3.	75	10	30	9	0.1	1.5
4.	65	15	45	7	0.3	1.5
5.	75	15	30	5	0.2	1.5
6.	75	5	30	5	0.2	1.5
7.	65	10	15	9	0.2	1.0
8.	75	15	30	9	0.2	1.5
9.	75	10	45	7	0.2	1.0
10.	65	5	45	7	0.3	1.5
11.	60	10	30	9	0.1	1.5
12.	60	5	30	5	0.2	1.5
13.	60	10	30	5	0.3	1.5
14.	60	10	30	9	0.3	1.5
15.	65	5	30	7	0.1	1.0
16.	65	10	30	7	0.2	1.5
17.	60	10	45	7	0.2	2.0
18.	65	5	30	7	0.3	2.0
19.	65	10	15	5	0.2	2.0
20.	60	5	30	9	0.2	1.5
21.	75	10	30	5	0.1	1.5
22.	65	15	15	7	0.1	1.5
23.	75	5	30	9	0.2	1.5
24.	75	10	30	5	0.3	1.5
25.	75	10	15	7	0.2	2.0
26.	65	10	15	9	0.2	2.0
27.	65	5	30	7	0.1	2.0
28.	65	10	45	5	0.2	2.0
29.	65	5	30	7	0.3	1.0
30.	65	15	30	7	0.1	1.0
31.	65	15	30	7	0.3	2.0
32.	65	10	30	7	0.2	1.5
33.	65	10	45	9	0.2	1.0

34.	60	10	15	7	0.2	1.0
35.	65	10	45	9	0.2	2.0
36.	65	10	45	5	0.2	1.0
37.	65	5	15	7	0.1	1.5
38.	75	10	15	7	0.2	1.0
39.	65	15	30	7	0.1	2.0
40.	65	15	15	7	0.3	1.5
41.	65	10	30	7	0.2	1.5
42.	75	10	30	9	0.3	1.5
43.	65	10	30	7	0.2	1.5
44.	65	10	30	7	0.2	1.5
45.	65	15	45	7	0.1	1.5
46.	60	15	30	5	0.2	1.5
47.	60	10	45	7	0.2	1.0
48.	65	15	30	7	0.3	1.0
49.	60	15	30	9	0.2	1.5
50.	65	10	30	7	0.2	1.5
51.	65	10	15	5	0.2	1.0
52.	60	10	15	7	0.2	2.0
53.	65	5	45	7	0.1	1.5
54.	60	10	30	5	0.1	1.5

Table 6: Process Variables and Their Corresponding Responses

Sl. No.	A Voltage (V)	B Current (A)	C Pulse ON (sec)	D Pulse OFF (sec)	E Gap (mm)	F Oil Pressure (Kg/cm²)	G MRR (Mg/sec)	H SR (µm)
1.	65	5	15	7	0.3	1.5	1.435	3.01
2.	75	10	45	7	0.2	2.0	5.800	6.09
3.	75	10	30	9	0.1	1.5	4.952	5.82
4.	65	15	45	7	0.3	1.5	8.823	6.86
5.	75	15	30	5	0.2	1.5	7.880	5.88
6.	75	5	30	5	0.2	1.5	2.083	4.43
7.	65	10	15	9	0.2	1.0	3.355	4.32
8.	75	15	30	9	0.2	1.5	7.960	5.22
9.	75	10	45	7	0.2	1.0	6.444	6.27
10.	65	5	45	7	0.3	1.5	2.653	6.16
11.	60	10	30	9	0.1	1.5	5.205	6.20
12.	60	5	30	5	0.2	1.5	1.990	4.41
13.	60	10	30	5	0.3	1.5	4.613	5.77
14.	60	10	30	9	0.3	1.5	4.511	6.41
15.	65	5	30	7	0.1	1.0	2.182	5.69
16.	65	10	30	7	0.2	1.5	4.951	5.39

17.	60	10	45	7	0.2	2.0	6.059	6.36
18.	65	5	30	7	0.3	2.0	2.136	4.35
19.	65	10	15	5	0.2	2.0	3.383	4.86
20.	60	5	30	9	0.2	1.5	2.206	4.91
21.	75	10	30	5	0.1	1.5	5.272	5.79
22.	65	15	15	7	0.1	1.5	5.342	3.12
23.	75	5	30	9	0.2	1.5	2.280	4.87
24.	75	10	30	5	0.3	1.5	4.951	6.17
25.	75	10	15	7	0.2	2.0	3.500	5.18
26.	65	10	15	9	0.2	2.0	3.248	5.14
27.	65	5	30	7	0.1	2.0	1.411	5.09
28.	65	10	45	5	0.2	2.0	5.544	7.44
29.	65	5	30	7	0.3	1.0	1.906	4.30
30.	65	15	30	7	0.1	1.0	7.381	6.39
31.	65	15	30	7	0.3	2.0	7.518	6.33
32.	65	10	30	7	0.2	1.5	5.272	5.10
33.	65	10	45	9	0.2	1.0	6.643	5.60
34.	60	10	15	7	0.2	1.0	3.383	3.74
35.	65	10	45	9	0.2	2.0	6.343	5.60
36.	65	10	45	5	0.2	1.0	6.766	8.19
37.	65	5	15	7	0.1	1.5	1.684	4.20
38.	75	10	15	7	0.2	1.0	2.859	5.31
39.	65	15	30	7	0.1	2.0	6.655	8.12
40.	65	15	15	7	0.3	1.5	3.866	4.01
41.	65	10	30	7	0.2	1.5	4.613	6.82
42.	75	10	30	9	0.3	1.5	4.142	7.08
43.	65	10	30	7	0.2	1.5	4.511	6.49
44.	65	10	30	7	0.2	1.5	4.720	6.51
45.	65	15	45	7	0.1	1.5	9.441	7.77
46.	60	15	30	5	0.2	1.5	6.766	7.70
47.	60	10	45	7	0.2	1.0	5.486	7.98
48.	65	15	30	7	0.3	1.0	5.205	8.02
49.	60	15	30	9	0.2	1.5	6.444	7.31
50.	65	10	30	7	0.2	1.5	3.941	5.01
51.	65	10	15	5	0.2	1.0	2.743	4.91
52.	60	10	15	7	0.2	2.0	2.985	4.97
53.	65	5	45	7	0.1	1.5	2.040	5.28
54.	60	10	30	5	0.1	1.5	4.776	6.54

- **Equation for MRR**

$$MRR = 1.6059+0.0852A-0.2872B-0.0740C-0.1632D-4.1745E-0.9694F - 0.0008A^2-0.0071B^2-0.00C^2+0.05D^2-7.6986E^2-0.4526F^2+0.0084AB+0.0006AC-0.0056AD -0.0663AE-0.0045AF+0.0125BC-0.0082BD-0.5275BE+0.1064BF +0.0008CD +0.1433CE -0.0197CF -0.6375DE + 0.0219DF+10.1EF$$

- **Equation for SR**

$$SR = 4.4805-0.1893A+1.2479B+0.6101C-0.4769D-41.5598E-3.2685F + 0.0021A^2-0.0163B^2-0.0023C^2+0.0165D^2+22.4167E^2 + 1.3300F^2 - 0.0116AB - 0.0043AC +0.0060AD+0.4410AE-0.0007AF+0.0038BC-0.0249BD + 0.1575BE+0.0295BF-0.0172CD+0.1058CE-0.0368CF+1.1625DE + 0.2025DF-6.9250EF$$

- A - Working Voltage
- B - Working Current
- C - Pulse ON Time
- D - Pulse OFF Time
- E - Spark Gap
- F - Oil Pressure

These relationships are derived through the utilization of Minitab software. Each and every one of the inherent qualities pertaining to exploration, as well as the projected values of information, are duly considered in order to conduct a comprehensive analysis for the purpose of identifying streamlined inputs. The aforementioned conditions are employed for the purpose of scrutinizing all the data in the MINITAB software, while the tabulated values pertain to the optimized characteristics of surface roughness and material removal rates.

Table 7: Result Obtained in Response Surface Methodology

Sl. No.	MRR (Mg/sec)	SR (µm)	Predicted MRR (Mg/sec)	Error MRR (Mg/sec)	Predicted SR (µm)	Error SR (µm)
1.	1.435	3.01	1.344776	-0.09022	3.087113	0.077113
2.	5.8	6.09	6.061756	0.261756	5.813608	-0.27639
3.	4.952	5.82	5.251514	0.299514	5.541237	-0.27876
4.	8.823	6.86	8.973476	0.150476	7.680313	0.820313
5.	7.88	5.88	7.859906	-0.02009	6.124508	0.244508
6.	2.083	4.43	1.970906	-0.11209	4.953008	0.523008
7.	3.355	4.32	3.160856	-0.19414	4.599508	0.279508
8.	7.96	5.22	7.552506	-0.40749	5.527908	0.307908
9.	6.444	6.27	6.375656	-0.06834	6.473108	0.203108
10.	2.653	6.16	2.740976	0.087976	5.119313	-1.04069
11.	5.205	6.2	5.020214	-0.18479	6.347487	0.147487
12.	1.99	4.41	2.133056	0.143056	4.587758	0.177758
13.	4.613	5.77	4.523526	-0.08947	6.079263	0.309263
14.	4.511	6.41	4.461126	-0.04987	6.085663	-0.32434
15.	2.182	5.69	2.530314	0.348314	5.174287	-0.51571

16.	4.951	5.39	4.661306	-0.28969	5.942458	0.552458
17.	6.059	6.36	5.660656	-0.39834	7.111108	0.751108
18.	2.136	4.35	2.182026	0.046026	4.482963	0.132963
19.	3.383	4.86	3.450356	0.067356	4.357608	-0.50239
20.	2.206	4.91	2.489656	0.283656	4.627158	-0.28284
21.	5.272	5.79	5.139914	-0.13209	6.104837	0.314837
22.	5.342	4.12	5.155064	-0.18694	4.953837	0.833837
23.	2.28	4.87	1.991506	-0.28849	5.352408	0.482408
24.	4.951	6.17	4.891926	-0.05907	6.236013	0.066013
25.	3.5	5.18	3.335956	-0.16404	5.370808	0.190808
26.	3.248	5.14	3.526756	0.278756	5.456008	0.316008
27.	1.411	5.09	1.014914	-0.39609	5.618787	0.528787
28.	5.544	7.44	5.948156	0.404156	7.122408	-0.31759
29.	1.906	4.3	1.677426	-0.22857	5.423463	1.123463
30.	7.381	6.39	7.410814	0.029814	6.702787	0.312787
31.	7.518	6.33	7.071526	-0.44647	6.621463	0.291463
32.	5.272	5.1	4.661306	-0.61069	5.942458	0.842458
33.	6.643	5.6	6.345656	-0.29734	6.404308	0.804308
34.	3.383	3.74	2.860256	-0.52274	4.278308	0.538308
35.	6.343	5.6	6.120556	-0.22244	6.156808	0.556808
36.	6.766	8.19	6.260856	-0.50514	8.179908	-0.01009
37.	1.684	4.2	1.617564	-0.06644	3.847837	-0.35216
38.	2.859	5.31	3.058856	0.199856	4.926308	-0.38369
39.	6.655	8.12	6.959414	0.304414	7.442287	-0.67771
40.	3.866	4.01	3.827276	-0.03872	4.508113	0.498113
41.	4.613	6.82	4.661306	0.048306	5.942458	-0.87754
42.	4.142	7.08	4.493526	0.351526	6.602413	-0.47759
43.	4.511	6.49	4.661306	0.150306	5.942458	-0.54754
44.	4.72	6.51	4.661306	-0.05869	5.942458	-0.56754
45.	9.441	7.77	9.441464	0.000464	7.491237	-0.27876
46.	6.766	7.7	6.762056	-0.00394	7.499258	-0.20074
47.	5.486	7.98	5.907056	0.421056	7.760108	-0.21989
48.	5.205	8.02	5.502926	0.297926	7.266963	-0.75304
49.	6.444	7.31	6.790656	0.346656	6.542658	-0.76734
50.	3.941	5.01	4.661306	0.720306	5.942458	0.932458
51.	2.743	4.91	3.172056	0.429056	4.311108	-0.59889
52.	2.985	4.97	3.204856	0.219856	4.733308	-0.23669
53.	2.04	5.28	2.153964	0.113964	5.245237	-0.03476
54.	4.776	6.54	4.572614	-0.20339	7.271087	0.731087

VIII. GREY RELATIONAL ANALYSIS

1. **Introduction to GRA**: In order to scrutinize the optimal selection of machining parameters for the process of Electrical Discharge Machining (EDM), the utilization of Gray Relational Analysis (GRA) is employed. The arrangement of a framework as posited by Gray theory entails a state of uncertainty or incompleteness in the model or the

information at hand. Furthermore, it demonstrates a proficient solution to the problem of uncertainty, multiple inputs, and discrete data. In accordance with the principles of the Taguchi quality plan concept, it was deemed prudent to employ an L32 mixed-orthogonal-array table for the purpose of conducting the investigations. Through the utilization of both Generalized Regression Analysis (GRA) and statistical methodology, it becomes apparent that the rate at which the table is fed exerts a discernible influence on the speed at which machining occurs. Additionally, the width of the gap and the duration of the heartbeat on time are observed to have an impact on the success rate (SR). Furthermore, through the establishment of an upper limit on the velocity of machining and a lower limit on the specific removal rate (SR), one can attain the most favorable machining parameters or achieve a targeted SR.

In the realm of antiquity, the intricate interplay between diverse factors alluded to remains shrouded in ambiguity. These entities are commonly referred to as "gray," denoting a state of ambiguity, insufficiency, and uncertainty in the realm of information. In the absence of substantial data sets, the application of conventional statistical techniques for analysis may be deemed inadequate or unreliable. In this endeavor, the objective was to transform the multi-reaction optimization model into a solitary reaction gray relational grade. To accomplish this, the researchers employed the utilization of GRA (Gray Relational Analysis). Grades are employed to focus on the multifaceted nature of multi-reaction characteristics, rather than employing experimental values directly in various regression models and genetic algorithms.

2. **Steps in GRA**: The below mentioned steps to be followed while applying grey relational analysis to find the Grey relational coefficients and the grey relational grade:

- Normalizing the experimental results of MRR and surface roughness to avoid the effect of adopting different units to reduce the variability.

$$Zij= \frac{yij-\min\,(yij,i=1,2,\ldots\ldots n)}{\max(yij,i=1,2\ldots\ldots n)-\min\,(yij,i=1,2\ldots\ldots n)} \quad (1)$$

$$Zij= \frac{\max(yij,i=1,2\ldots\ldots n)-yij}{\max(yij,i=1,2\ldots\ldots n)-mi\quad(yij,i=1,2\ldots\ldots n)} \quad (2)$$

- Performing the grey relational generating and calculating the grey coefficient for the normalized values yield.

$$\gamma(y0(k),yi(k))= \frac{\Delta\min+\xi\Delta\max}{\Delta oj(k)+\xi\Delta\max} \quad (3)$$

Where,

- j=1, 2...n; k=1, 2...m, n is the number of experimental data items and m is the number of responses.
- y0(k) is the reference sequence (yo(k)=1, k=1, 2...m); yj(k) is the specific comparison sequence.

- $\Delta oj = \| yo(k) - yj(k) \|$ = The absolute value of the difference between y0(k) and yj(k).
- $\Delta min = \min\min \| yo(k) - yj(k) \|$ is the smallest value of yj(k).
- $\Delta max = \max\max \| yo(k) - yj(k) \|$ is the largest value of yj(k).
- ζ is the distinguishing coefficient which is defined in the range $0 \leq \zeta \leq 1$ (the value may adjusted based on the practical needs of the system).

- Calculating the grey relational grade by averaging thegrey relational coefficient yields:

$$\gamma j = \frac{1}{k} \sum \gamma ij \qquad (4)$$

In the given context, γj represents the grey relational grade assigned to the jth experiment, while k denotes the total number of performance characteristics being considered. In order to standardize the experimental value, Equation (1) is employed, particularly when the objective of the initial value exhibits the characteristic of 'greater is preferable'. The equation provided above is utilized to standardize the Mean Reciprocal Rank (MRR). When the attribute of the original sequence is defined by the principle of "lower the better," the original sequence is subjected to normalization using Equation (2). In other words, the equation mentioned is employed to normalize the surface roughness. By employing Equation (3), we proceed to compute the grey relational coefficient pertaining to the Material Removal Rate (MRR) and Surface Roughness (SR), as exemplified in Table 2. Furthermore, the computation of the grey relational grade is performed in accordance with Equation (4).

Table 8: Grey Relational Grade

Sl. No.	Normalized Values for MRR	Normalized Values for SR	GRC Values for MRR	GRC Values for SR	Grade
1.	0	1	0.333	0.4169	0.6665
2.	0.5452	0.405	0.523	0.4393	0.4699
3.	0.4394	0.457	0.4714	0.3641	0.4553
4.	0.923	0.257	0.8665	0.4344	0.6153
5.	0.805	0.446	0.7194	0.6100	0.5769
6.	0.08	0.728	0.3521	0.6234	0.4810
7.	0.239	0.747	0.3965	0.4991	0.5099
8.	0.815	0.573	0.7299	0.4035	0.6145
9.	0.625	0.371	0.5714	0.4117	0.4874
10.	0.152	0.392	0.3709	0.4085	0.3973
11.	0.470	0.384	0.4854	0.6109	0.4469
12.	0.069	0.729	0.3494	0.4439	0.4801
13.	0.396	0.461	0.4528	0.3891	0.4483
14.	0.384	0.332	0.4480	0.4514	0.4185
15.	0.093	0.483	0.3553	0.4805	0.4033
16.	0.439	0.540	0.4712	0.4838	0.4758

17.	0.652	0.546	0.5896	0.6216	0.4367
18.	0.087	0.741	0.3538	0.5438	0.4477
19.	0.243	0.643	0.3977	0.4939	0.4707
20.	0.096	0.564	0.3561	0.4221	0.4250
21.	0.479	0.463	0.4897	0.6654	0.4659
22.	0.488	0.786	0.4940	0.5424	0.5797
23.	0.105	0.641	0.3584	0.4105	0.5404
24.	0.439	0.389	0.4712	0.5038	0.4408
25.	0.257	0.581	0.4022	0.5087	0.4530
26.	0.226	0.589	0.3924	0.5142	0.4505
27.	0.089	0.598	0.3543	0.3323	0.4343
28.	0.4173	0.145	0.4618	0.6308	0.3970
29.	0.058	0.751	0.3467	0.3945	0.4887
30.	0.7426	0.347	0.6601	0.3989	0.5273
31.	0.759	0.359	0.6747	0.5129	0.5365
32.	0.479	0.596	0.4897	0.4597	0.5013
33.	0.65	0.5	0.5882	0.7511	0.5239
34.	0.243	0.859	0.3977	0.5497	0.5744
35.	0.613	0.5	0.5636	0.2985	0.5116
36.	0.665	0	0.5988	0.6491	0.4486
37.	0.311	0.77	0.3403	0.4894	0.4947
38.	0.177	0.556	0.3779	0.3012	0.4346
39.	0.652	0.013	0.5896	0.6879	0.4454
40.	0.303	0.807	0.4177	0.3663	0.5528
41.	0.396	0.264	0.4528	0.3512	0.4095
42.	0.3381	0.214	0.4303	0.6332	0.3857
43.	0.3842	0.328	0.4481	0.3863	0.5406
44.	0.4103	0.324	0.4588	0.3165	0.4225
45.	1	0.081	1	0.3196	0.6582
46.	0.665	0.094	0.5988	0.3071	0.4592
47.	0.505	0.040	0.5025	0.3056	0.4048
48.	0.470	0.033	0.4854	0.3338	0.3955
49.	0.625	0.151	0.5714	0.5243	0.4526
50.	0.313	0.614	0.4212	0.5369	0.4727
51.	0.163	0.633	0.3739	0.5245	0.4554
52.	0.193	0.622	0.3825	0.4928	0.4560
53.	0.075	0.562	0.3508	0.3842	0.4212
54.	0.4173	0.318	0.4618	0.3841	0.4230

IX. ARTIFICIAL NEURAL NETWORKS ARCHITECTURE

The artificial neural network (ANN) primarily consists of multiple layers, each serving a distinct purpose. The initial layer, referred to as the information layer, is responsible for applying intricate patterns to the input data. Subsequently, the outcome layer, positioned at the end of the network, receives and processes the final result. The intermediate layers, situated between the information and outcome layers, are known as the hidden layers, as

depicted in Figure 7. There exist one or more clandestine strata, aptly denominated as such due to their outcomes eluding direct detection. When the magnitude of the input layer reaches a substantial level, the inclusion of additional hidden layers enables the neural network to extract higher-order insights that are predominantly significant. The concept at hand pertains to the state of being either fully or partially interconnected. Neuronal layers are characterized by their ongoing and subsequent arrangement of interconnected neurons, wherein each interconnection exhibits a corresponding association strength, commonly referred to as weight. In the context of a progressive trajectory, the transmission of the information signal occurs within the network, following a sequential layering approach commonly referred to as Multilayer Perceptrons (MLP). A multitude of distributions scrutinize the progression and speculation surrounding Artificial Neural Networks (ANN).

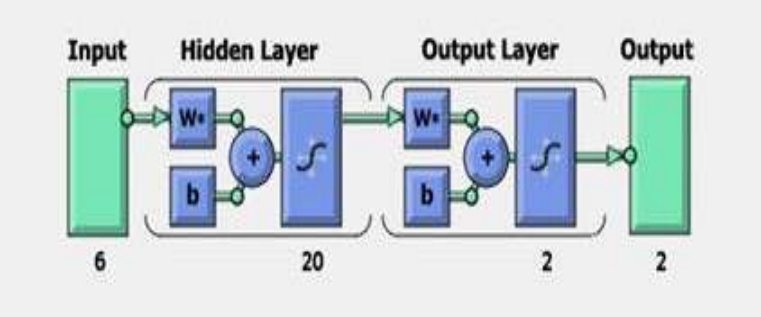

Figure 7: General Configuration of Artificial Neural Network

To iteratively minimize the following cost function, the back-propagation training algorithm is commonly used, with respect to the interconnection weights and neurons three sholds:

$$\mathbf{E} = \frac{\mathbf{1}}{\mathbf{2}} \sum_{\mathbf{1}}^{\mathbf{P}} \sum_{\mathbf{i=0}}^{\mathbf{N}} (\mathbf{d_i} - \mathbf{o_i})^{\mathbf{2}} \qquad (5)$$

Where P is the number of training input/output patterns and N is the number of output nodes. d_i and O_i are the target and actual responses for output node i respectively. Iteratively, the interconnection weights between the j_{th} node and the i_{th} node are updated as:

$$\mathbf{W_{ij}(t+1)} = \boldsymbol{\alpha} \mathbf{w_{ji}(t)} + \boldsymbol{\eta} \mathbf{x_i f'\left(net_j^k\right)} \sum_{\mathbf{i=1}}^{\mathbf{N}} (\mathbf{d_i} - \mathbf{O_i}) \mathbf{f'(net_i^0) w_{ij}} \qquad (6)$$

Let us consider a scenario where "a" represents a constant denoting momentum, "g" symbolizes the learning rate, "xi" signifies the input pattern at the iterative sample "t", "net0N" represents the input to node "N" at the output layer, and "netkj" denotes the input to a node "j" in the "kth" layer. The learning rate parameter governs the degree of sensitivity to errors in relation to weight adjustments, thereby determining the magnitude of weight correction. The velocity of convergence and the stability of weights are subject to alteration during the process of learning. The existence of an optimal learning rate is contingent upon

the specific attributes of the error surface. A diminutive rate is deemed preferable for surfaces that exhibit swift alterations, whereas an augmented value of the learning rate shall expedite the process of convergence for surfaces that possess a seamless nature. The consistent momentum, typically ranging from 0.1 to 1, serves to facilitate the refinement of weight updates and prevent undesirable oscillations within the system. Moreover, it enables the system to transcend local minima during the training process by reducing its susceptibility to localized alterations. Much like the learning rate, the optimal value of the momentum constant is idiosyncratic to the particular contours of the error surface.

The training process is deemed complete once the Mean-Square-Error (MSE), Root-Mean-Square-Error (RMSE), or Normalized-Mean-Square-Error (NMSE) between the empirical data and the outcomes generated by the Artificial Neural Network (ANN) for all elements in the training set has surpassed a predetermined threshold, or alternatively, when the specified number of learning epochs has been reached.

The divergent nature of input requirements and modeling capabilities necessitates a distinction, despite the shared operational characteristics among all neural network models. Henceforth, it is imperative to acknowledge that each paradigm inherently harbors advantages and disadvantages contingent upon its specific application. Therefore, the judicious selection of an appropriate network class, accompanied by suitable parameters, becomes paramount in ensuring the triumph of an application.

1. **Back-Propagation Network Algorithm:** The algorithm for the back-propagation network program is depicted below with the support of flow diagram as shown in Figure 8.

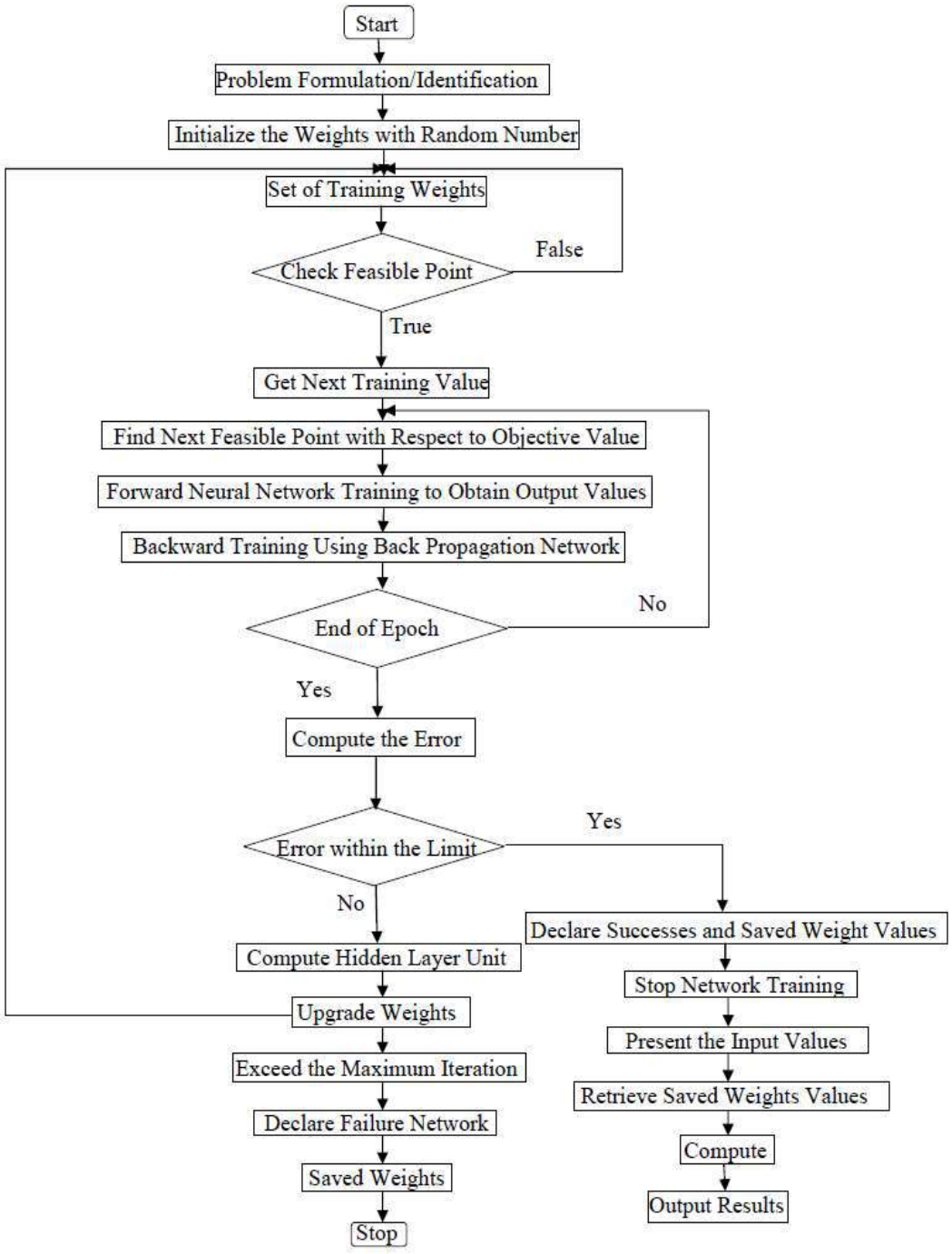

Figure 8: Back-Propagation Network Program

- **Step 1:**Confirm the number of hidden layers.

- **Step 2:**Confirm the neurons number for the input layer and the output layer. For the input layer, the neurons number equalizes the number of input variables and for the output layer it equalizes the number of outputs required. Set few neurons number for the hidden layer.

- **Step 3:**Get the training input pattern.

- **Step 4:**Assign small weight values for the neurons interconnected between the input, hidden and output layers.

- **Step 5:**Calculate the output values for all the neurons in hidden and output layers using the following formula.

$$\mathbf{out_i = f(\sum_{wij} Out_j + \theta_1} \quad (7)$$

Where $output_i$ is the output of the i^{th} neuron in the layer under consideration; $output_j$ is the output of the j^{th} neuron in the preceding layer. f is the sigmoid function can be expressed as:

Where q is termed as temperature.

- **Step 6:** Determine the output at the output layer and compare it with the desired output values.

$$\mathbf{f(net_1)} = \frac{1}{1+e^{-net\, i/q}} \quad (8)$$

Determine the error of the output neurons,

$$\text{Error} = \text{desired output} - \text{actual output} \quad (9)$$

Similarly, determine the root mean square error value of the output neurons.

- **Step 7:** Determine the error existing at the neurons of the hidden layer and back-propagate those errors to the weight values connected in between the neurons of the hidden layer and input layer. Similarly, back propagate the errors available at the output neurons to the weight values connected in between the neurons of the hidden layer and output layer using the following formula.

$$\mathbf{E_p} = \frac{1}{2}\sum(t_{pj} - O_{pj})^2 \quad (10)$$

Where E_p is the error for the p^{th} presentation vector, t_{pj} is the desired value for the j^{th} output neuron and O_{pj} is the desired output of the j^{th} output neuron.

$$\text{error } \delta_{pi} = (t_{pi} - O_{pi})O_{pi}(1 - O_{pi}) \quad (11)$$

for output neurons,

$$\text{error}\,\delta_p = (t_{pi} - O_{pi})O_{pi}\sum \delta_{pi}W_{ki} \tag{12}$$

for hidden neurons Weight adjustment is made as follows:

$$\Delta W_{ji}(n=1) = \eta(\delta_{pi}O_{pi}) = \alpha\,\Delta W_{ji}(n) \tag{13}$$

Where η is the learning rate parameter and α is momentum factor.

- **Step 8:** Go to **Step 3** and do the calculations up to **Step 7** at the end of cycle determine the root-mean-square error value, mean percentage of error and worst percentage of error over the complete patterns. To reach to **Step 9** check for reasonable error, if so, go to Step 9 otherwise go to **Step 3** and repeat the same from **Step 3** to **Step 7**.

- **Step 9:** Stop the iteration and note the final weight values of the hidden layer neurons and also to the output layer neurons.

- **Step 10:** Testing neural network model with the trained weight values, determine the output for the testing pattern and check whether the deviation from desired value is reasonably less or not. If not, try the back propagation with revised network by modifying the number of neurons, varying learning rate parameters, momentum value and temperature values as well. Table 9 shows the typical observation of network performance while testing the pattern.

Table 9: Results Obtained in Artificial Neural Network

Sl. No.	MRR (Mg/sec)	SR (µm)	Predicted MRR (Mg/sec)	Predicted SR (µm)
1.	1.435	3.01	1.435	3.01
2.	5.8	6.09	5.8	6.09
3.	4.952	5.82	4.957	5.82
4.	8.823	6.86	8.823	6.85
5.	7.88	5.88	7.88	5.88
6.	2.083	4.43	2.085	4.43
7.	3.355	4.32	3.355	4.32
8.	7.96	5.22	7.96	5.22
9.	6.444	6.27	6.444	6.25
10.	2.653	6.16	2.653	6.16
11.	5.205	6.2	5.205	6.2
12.	1.99	4.41	1.99	4.41
13.	4.613	5.77	4.613	5.77
14.	4.511	6.41	4.511	6.41

15.	2.182	5.69	2.182	5.68
16.	4.951	5.39	4.954	5.39
17.	6.059	6.36	6.059	6.34
18.	2.136	4.35	2.136	4.35
19.	3.383	4.86	3.383	4.86
20.	2.206	4.91	2.205	4.93
21.	5.272	5.79	5.272	5.79
22.	5.342	4.12	5.342	4.12
23.	2.28	4.87	2.28	4.86
24.	4.951	6.17	4.951	6.17
25.	3.5	5.18	3.5	5.18
26.	3.248	5.14	3.245	5.15
27.	1.411	5.09	1.411	5.09
28.	5.544	7.44	5.545	7.45
29.	1.906	4.3	1.908	4.3
30.	7.381	6.39	7.384	6.36
31.	7.518	6.33	7.518	6.33
32.	5.272	5.1	5.272	5.1
33.	6.643	5.6	6.643	5.6
34.	3.383	3.74	3.383	3.75
35.	6.343	5.6	6.343	5.6
36.	6.766	8.19	6.766	8.19
37.	1.684	4.2	1.687	4.2
38.	2.859	5.31	2.859	5.31
39.	6.655	8.12	6.655	8.12
40.	3.866	4.01	3.866	4.01
41.	4.613	6.82	4.613	6.82
42.	4.142	7.08	4.144	7.07
43.	4.511	6.49	4.511	6.49
44.	4.72	6.51	4.72	6.51
45.	9.441	7.77	9.441	7.77
46.	6.766	7.7	6.766	7.7
47.	5.486	7.98	5.488	7.99
48.	5.205	8.02	5.205	8.02
49.	6.444	7.31	6.444	7.31
50.	3.941	5.01	3.941	5.01
51.	2.743	4.91	2.743	4.91
52.	2.985	4.97	2.985	4.97
53.	2.04	5.28	2.04	5.28
54.	4.776	6.54	4.776	6.54

X. RESULT AND DISCUSSION FOR MRR AND SR

The symmetrical exhibit was arranged by utilizing Focal Composite Design of 54 runs. The Focal Composite Design, Response Surface Methodology, Contour plots and Optimization plots are framed by utilizing MINITAB Software. Figure 9 addresses MRR as an element of heartbeat off time and heartbeat on time, though the Voltage, current, hole width and Poil stays steady in its more significant level. It is seen as the most elevated MRR values happened at the higher heartbeat on time and lower beat off time. Figure 10 shows MRR as an element of heartbeat on time and voltage, though the current, hole width, Poil and beat off time stay consistent in its more elevated level. It shows that the most elevated MRR values happened at the higher heartbeat on time and lower voltage. Figure 11 addresses SR as a component of current and hole width, while the voltage, beat on time, beat off time and oil pressure stays steady in its more significant level. It shows that the most noteworthy SR values happened at the greatest current and lower hole width.

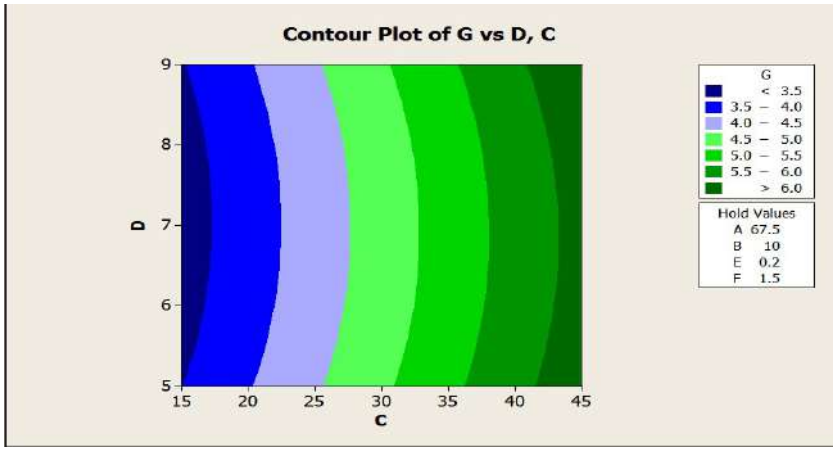

Figure 9: MRR as a Function of Pulse OFF Time and Pulse ON Time

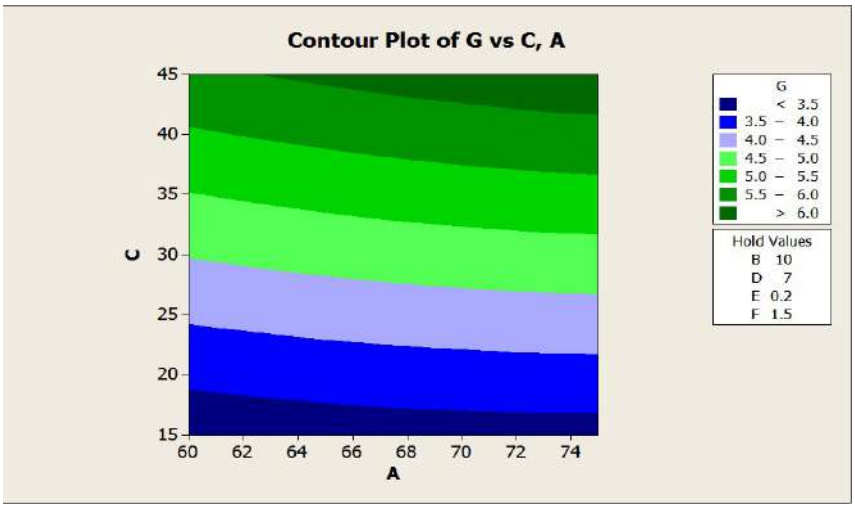

Figure 10: MRR as a Function of Pulse OFF Time and Voltage

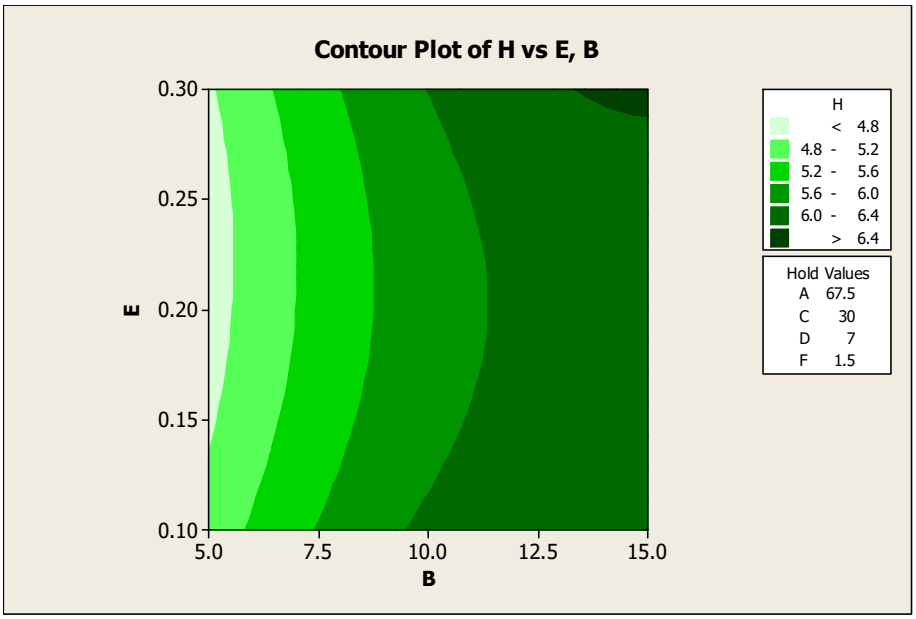

Figure 11: SR as a Function of Current and Gap Width

Figure 12 represents SR as a function of voltage and pulse off time, whereas the current, pulse off, voltage, gap width and P_{oil} remains constant in its higher level. It is observed that the highest SR values occurred at the minimum voltage and minimum gap width value. Figure 13 represents SR as a function of pulse on time and pulse off time, whereas the voltage, gap width, current and P_{oil} remains constant in its higher level. It's observed that the highest SR values occurred at the higher pulse off time and lower pulse on time.

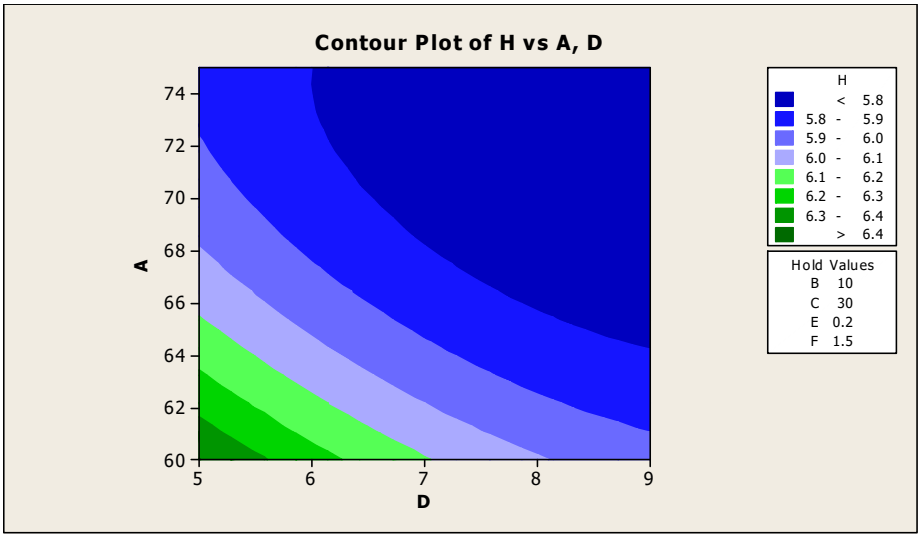

Figure 12: SR as a Function of Voltage and Pulse OFF Time

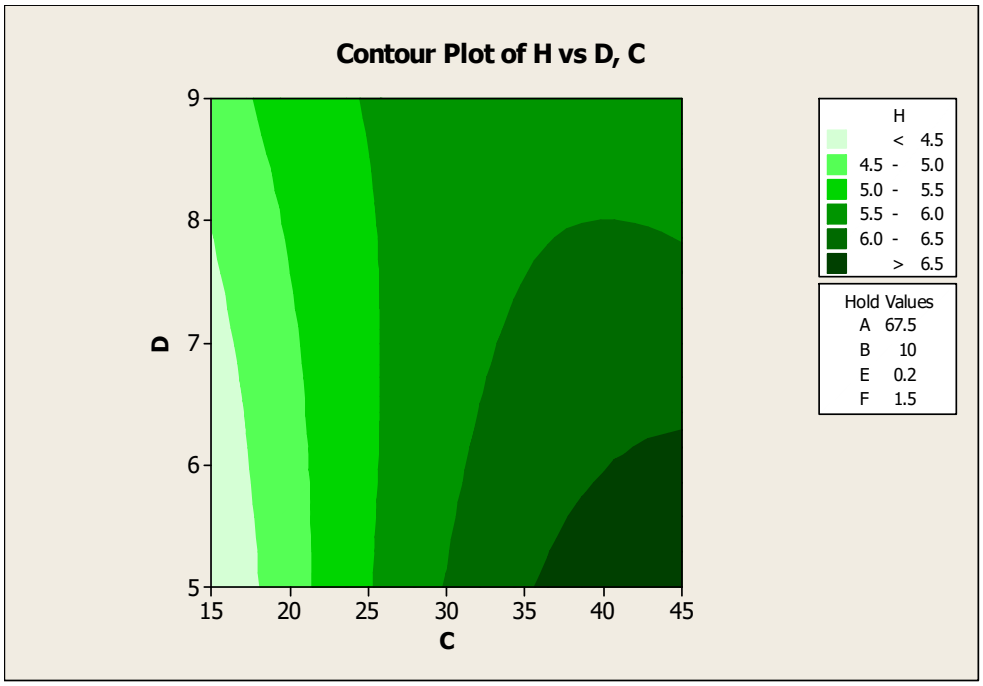

Figure 13: SR as a Function of Pulse ON Time and Pulse OFF Time

The bar outline for MRR and SR are displayed in Figure 14 and 15 alongside the different boundaries utilizing RSM and ANN. The ANN is prepared with different quantities of hubs in the secret layer. 10 secret layers are acquired from the specific hubs. The thought process in involving two secret layer and 10 hubs in this arrangement is because of diminished blunder. The Typical blunder for the performance of ANN during testing of all the preparation and it is 1.47% to test design. ANN is a fitting apparatus, utilized in ascertaining the material removal rate and surface roughness in machining process. ANN model has been tried utilizing the preparation information and bar outlines were not set in stone and tried values.

The outcomes illustrate that ANN model has been effectively applied to the machining boundaries of LM25 Aluminum composites. It is seen from Figure 14 (Validation of ANN and RSM model for SR) Figure 15 (Validation of ANN and RSM model for MRR) that anticipated in view of ANN model is extremely near the trial perception. The validation for the MRR SR values utilizing ANN has been recorded in Table 4. The level of blunder between the trial and anticipated values is tracked down that base of 0.30 and limit of 3.22. This mistake is a sensible one and shows that the ANN model anticipated palatable for MRR and SR.

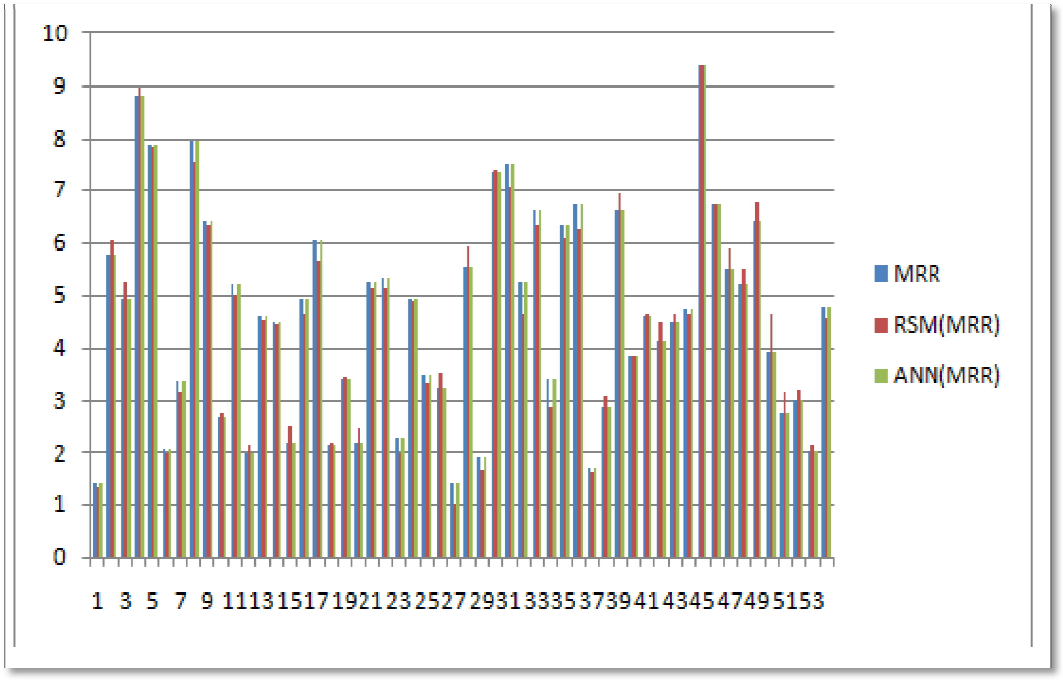

Figure 14: Variation of MRR and MRR Output of Training Data Set w.r.t RSM

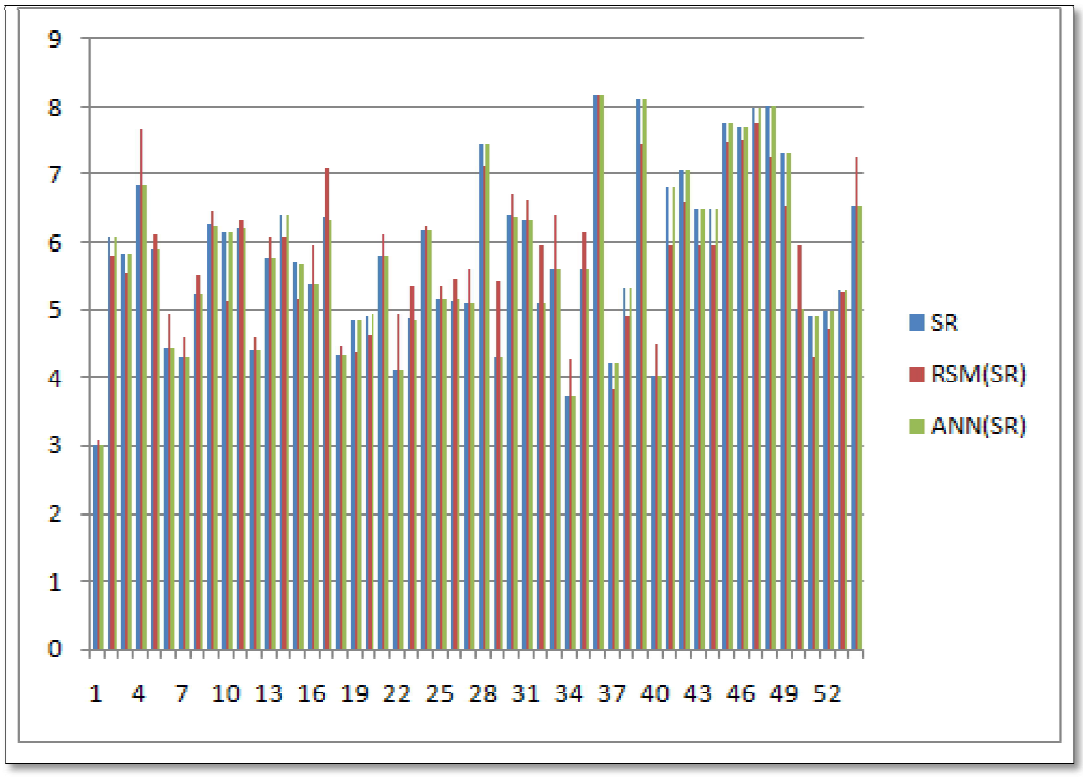

Figure 15: Variation of SR and SR Output of Training Data Set w.r.t RSM

XI. CONCLUSION

In this work, the information parameters are Discharge Current, Discharge Voltage, Pulse ON time, Pulse OFF Time, gap width, Oil Pressure and Metal Removal Rate, Surface Roughness are the output machining parameters. Different degrees of information conditions are consequential of Surface Design of Experiments. The experiments are performed on Electrical Discharge Machining machine. Utilizing the exploratory outcomes, two models viz., the Response Surface Methodology and Artificial Neural Networks are made and determined. The last conclusions in view of these two prediction models, the ANN back propagation strategy with a sort of observational model gives great outcome when contrasted and RSM model and the upgraded boundary for this composition are given in table 10.

A Voltage (V)	B Current (A)	C Pulse ON (sec)	D Pulse OFF (sec)	E Gap (mm)	F Oil Pressure (Kg/cm^2)	G MRR (Mg/sec)	H SR (µm)
65	15	15	7	0.1	1.5	5.342	3.12

REFERENCES

[1] Kuldeep Ojha, R. K. Garg, Singh.K. K. (2010). MRR Improvement in Sinking Electrical Discharge Machining, A Review Journal of Minerals and Materials Characterization and Engineering, 9, (8), 709-739.
[2] Sen. M, Shan. H. S. (2007). Electro Jet Drilling Using Hybrid NNGA Approach, International Journal Robot and Computer Integrated Manufacturing, 23, 17–24.
[3] Gao. Q, Zhang. Q. H, Su. S. P, Zhang. J. H. (2008). Parameter Optimization Model In Electrical Discharge Machining Process, Journal of Zhejiang University Science, A9, (1), 104–108.
[4] Rao. G. K. M, Janardhana. G. R, Rao. D. H, Rao. M. S. (2009). Development of Hybrid Model and Optimization of Surface Roughness in Electric Discharge Machining Using Artificial Neural Networks and Genetic Algorithm, Journal of Material Processing Technology,.209, 1512–1520.
[5] Tolga Bozdana. A, Oguzhan Yilmaz, Ali Okka. M, Huseyin Filiz. I. (2010). Mathematical Modelling of EDM Hole Drilling Using Response Surface Methodology, Department of Mechanical Engineering, The University of Gaziantep, 27310, Gaziantep, Turkey 90 – 94.
[6] Musrrat Ali, Millie Pant, and Singh. V. P. (2009). An Improved Differential Evolution Algorithm for Real Parameter Optimization Problems, International Journal of Recent Trends in Engineering, 1, (5).
[7] Yan. B. H, Huang. F. Y, Chow. H. M, Tsai. J. Y. (1999). Micro-Hole Machining of Carbide by Electric Discharge Machining, Journal Materials Processing Technology, 87, 139–145.
[8] Mahapatra.S and Amar Patnaik. (2006). Parametric Optimization of Wire Electrical Discharge Machining Process using Taguchi Method, Journal of the Brazilian Society of Mechanical Sciences and Engineering, 28(4) 422-429.
[9] Qing Gao, Qin-He Zhang, Shu-peng SU, Jian-hua Zhang.(2008). Parameter Optimization Model in Electrical Discharge Machining Process, Journal of Zhejiang University Science A, 9(1), 104-108.
[10] Shabgard M. R, Shotorbani. R. M, (2009). Mathematical Modeling of Machining Parameters in Electrical Discharge Machining of FW4 Welded Steel, World Academy of Science, Engineering and Technology, 52.
[11] Sushant Dhar, Rajesh Purohit, Nishant Saini, Akhil Sharma, Hemath Kumarb. G. (2007). Mathematical Modeling of Electric Discharge Machining of Cast Al–4Cu–6Si alloy–10 wt.% SiC_p Composites, Journal of Materials Processing Technology, 194, 24–29.
[12] Puertas. I, LuisA. C. J. (2003). Study on the Machining Parameters Optimization of EDM, Journal of Materials Processing Technology, 143–144, 521–526.

[13] Thillaivanan. A, Asokan. P, Srinivasan. K. N and Saravanan. R. (2010). Optimization of Operating Parameters for EDM Process Based on the Taguchi Method and Artificial Neural Network, International Journal of Engineering Science and Technology, 2, (12), 6880-6888.
[14] Sameh S. Habib. (2009). Study of the Parameters in EDM Through Response Surface Methodology Approach, Applied Mathematical Modeling, 33, 4397–4407.
[15] Seung-Han Yanga, Srinivas .J, Sekar Mohana, Dong-Mok Leea, Sree Balaji B. (2009). Optimization of Electric Discharge Machining Using Simulated Annealing, Journal of Materials Processing Technology, 209, 4471–4475.
[16] Ramezan Ali MahdaviNejad. (2011). Modeling and Optimization of EDM of SiC Parameters, Using Neural Network and Non-dominating Sorting Genetic Algorithm (NSGA II), Materials Sciences and Applications, 2, 669-675.
[17] Krishna Mohana Rao. G and Hanumantha Rao. D. (2010). Hybrid Modeling and Optimization of Hardness of Surface Produced by Electric Discharge Machining Using Artificial Neural Networks and Genetic Algorithm, Journal Engineering and Applied Sciences, 5, (5), 1819-6608.
[18] Majumder, Arindam. (2012). Parametric Optimization of Electric Discharge Machining by GA-Based Response Surface Methodology, Journal for Manufacturing Science and Production, 12, (12), 25–30.
[19] Jun Wang, Fei Yang, Jun Qian, Dominiek Reynaerts. (2016). Study of alternating current flow in micro-EDM through real time pulse counting, Journal of Materials Processing Technology (231) 179–188.

